

**MEASUREMENT OF MULTIJET CROSS-SECTION RATIOS IN  
PROTON-PROTON COLLISIONS WITH THE CMS DETECTOR AT  
THE LHC**

A THESIS

Submitted to the  
FACULTY OF SCIENCE  
PANJAB UNIVERSITY, CHANDIGARH  
for the degree of

**DOCTOR OF PHILOSOPHY**

**2017**

**Anterpreet Kaur**

DEPARTMENT OF PHYSICS  
CENTRE OF ADVANCED STUDY IN PHYSICS  
PANJAB UNIVERSITY, CHANDIGARH  
INDIA



*Dedicated to  
my Grand-Parents*

*&*

*Parents*









# Contents

List of Figures	xii
-----------------	-----

List of Tables	xiii
----------------	------

---

1 Measurement of the Differential Inclusive Multijet Cross Sections and their Ratio	1
1.1 Data Samples . . . . .	2
1.1.1 Monte Carlo samples . . . . .	3
1.2 Event Selection . . . . .	4
1.2.1 Certified Data . . . . .	4
1.2.2 Trigger Selection . . . . .	4

List of publications	9
----------------------	---

Reprints	11
----------	----







# List of Figures

1.1	Trigger efficiencies turn-on curves for the single jet trigger paths used in the analysis. . . . .	6
-----	---	---



# List of Tables

1.1	Four data sets collected in run periods A, B,C and D during 2012, along with the corresponding run numbers and luminosity. . . . .	2
1.2	The official MC production samples generated in phase space slices in $H_T$ with the generator MADGRAPH5 and interfaced to PYTHIA6 for the parton shower and hadronization of the events. The cross section and number of events generated are mentioned for each sample. . . .	4
1.3	HLT trigger thresholds and corresponding L1SingleJet trigger. . . . .	5

# Chapter 1

## Measurement of the Differential Inclusive Multijet Cross Sections and their Ratio

The inclusive  $n$ -jet event samples include the events with number of jets  $\geq n$ , where  $n = 2$  and 3 in the current study. The inclusive multijet event yields are transformed into a differential cross section which is defined as :

$$\frac{d\sigma}{d(H_{T,2}/2)} = \frac{1}{\epsilon \mathcal{L}_{\text{int,eff}}} \frac{N_{\text{event}}}{\Delta(H_{T,2}/2)} \quad (1.1)$$

where  $N_{\text{event}}$  is the number of inclusive 2- or 3-jet events counted in an  $H_{T,2}/2$  bin,  $\epsilon$  is the product of the trigger and jet selection efficiencies, which are greater than 99%,  $\mathcal{L}_{\text{int,eff}}$  is the effective integrated luminosity, and  $\Delta(H_{T,2}/2)$  are the bin widths. The measurements are reported in units of (pb/GeV).

The differential inclusive multijet cross sections are measured as a function of the average transverse momentum,  $H_{T,2}/2 = \frac{1}{2}(p_{T,1} + p_{T,2})$ , where  $p_{T,1}$  and  $p_{T,2}$  denote the transverse momenta of the two leading jets. The cross section ratio  $R_{32}$ , defined in Eq. 1.2 is obtained by dividing the differential cross sections of inclusive 3-jet

events to that of inclusive 2-jet one, for each bin in  $H_{T,2}/2$ .

$$R_{32} = \frac{\frac{d\sigma_{3-jet}}{d(H_{T,2}/2)}}{\frac{d\sigma_{2-jet}}{d(H_{T,2}/2)}} \quad (1.2)$$

For inclusive 2-jet events ( $n_j \geq 2$ ) sufficient data are available up to  $H_{T,2}/2 = 2$  TeV, while for inclusive 3-jet events ( $n_j \geq 3$ ) and the ratio  $R_{32}$ , the accessible range in  $H_{T,2}/2$  is limited to  $H_{T,2}/2 < 1.68$  TeV.

## 1.1 Data Samples

This measurement uses the data collected at the center of mass energy of 8 TeV by CMS experiment in the 2012 run period of the LHC. The 2012 data is taken in four periods A, B, C, D and the data sets are divided into samples according to the run period. Further each sample is grouped into subsets based on the trigger decision. For run B-D, the **JetMon** stream datasets contain prescaled low trigger threshold paths (HLTPFJet40, 80, 140, 200 and 260) while the **JetHT** stream datasets contain unprescaled high threshold trigger paths (HLT PFJet320 and 400). For run A, the **Jet** stream contains all the above mentioned trigger paths. The datasets used in the current study are mentioned in the Table 1.1 along with the luminosity of each dataset :

Table 1.1: Four data sets collected in run periods A, B,C and D during 2012, along with the corresponding run numbers and luminosity.

Run	Run range	Data set	Luminosity $\text{fb}^{-1}$
A	190456-193621	/Jet/Run2012A-22Jan2013-v1/AOD	0.88
B	193834-196531	/Jet[Mon,HT]/Run2012B-22Jan2013-v1/AOD	4.41
C	198022-203742	/Jet[Mon,HT]/Run2012C-22Jan2013-v1/AOD	7.06
D	203777-208686	/Jet[Mon,HT]/Run2012D-22Jan2013-v1/AOD	7.37

The data sets have the LHC luminosity increasing with period, full data sample of 2012 corresponds to an integrated luminosity of  $19.71 \text{ fb}^{-1}$ .

### 1.1.1 Monte Carlo samples

To have a comparison of data results with the simulated events, the MADGRAPH5 [1] Monte-Carlo event generator has been used. The MADGRAPH5 generates matrix elements for High Energy Physics processes, such as decays and  $2 \rightarrow n$  scatterings. The underlying event is modeled using the tune Z2\*. It has been interfaced to PYTHIA6 [2] by the LHE event record [3], which generates the rest of the higher-order effects using the Parton Showering (PS) model. Matching algorithms ensure that no double-counting occurs between the tree-level and the PS-model-generated partons. The MC samples are processed through the complete CMS detector simulation to allow studies of the detector response and compare to measured data on detector level.

The cross section measured as a function of the transverse momentum  $p_T$  or the scalar sum of the transverse momentum of all jets  $H_T$  falls steeply with the increasing  $p_T$ . So in the reasonable time, it is not possible to generate a large number of high  $p_T$  events. Hence, the events are generated in the different phase-space region binned in  $H_T$  or the leading jet  $p_T$ . Later on, the different phase-space regions are added together in the data analyses by taking into account the cross section of the different phase-space regions. The official CMS MADGRAPH5 + PYTHIA6 MC samples used in this analysis are generated as slices in the  $H_T$  phase-space are tabulated in Table 1.2 along with their cross sections and number of events generated.



Table 1.2: The official MC production samples generated in phase space slices in  $H_T$  with the generator MADGRAPH5 and interfaced to PYTHIA6 for the parton shower and hadronization of the events. The cross section and number of events generated are mentioned for each sample.

Generator	Sample	Events	Cross Section pb
MADGRAPH5 + PYTHIA 6	/QCD_HT-100To250_TuneZ2star_8TeV-madgraph-pythia6/ Summer12_DR53X-PU_S10_START53_V7A-v1/AODSIM	50129518	$1.036 \times 10^7$
	/QCD_HT-250To500_TuneZ2star_8TeV-madgraph-pythia6/ Summer12_DR53X-PU_S10_START53_V7A-v1/AODSIM	27062078	$2.760 \times 10^5$
	/QCD_HT-500To1000_TuneZ2star_8TeV-madgraph-pythia6/ Summer12_DR53X-PU_S10_START53_V7A-v1/AODSIM	30599292	$8.426 \times 10^3$
	/QCD_HT-1000ToInf_TuneZ2star_8TeV-madgraph-pythia6/ Summer12_DR53X-PU_S10_START53_V7A-v1/AODSIM	13843863	$2.040 \times 10^2$

## 1.2 Event Selection

To yield a multijet sample with high purity and high selection efficiency, the events are selected according to several quality criteria. This event selection also reduces beam induced background, detector-level noise and jets arising from fake calorimeter energy deposits.

### 1.2.1 Certified Data

### 1.2.2 Trigger Selection

The CMS Trigger and Data Acquisition System (TriDAS) is designed to inspect the detector information at the full crossing frequency and to select events at a maximum rate of  $O(10^2)$  Hz for archiving and later offline analysis. The required rejection rate of  $O(10^5)$  Hz is too large to be achieved in a single processing step, if a high efficiency is to be maintained for the physics phenomena, CMS plans to study. For this reason, the full selection task is split into two steps : Level-1 Trigger, (L1 - hardware trigger) and Higher Level Trigger, (HLT - software trigger).

In this analysis the trigger paths which are used are single jet triggers which consists of one L1 trigger seed and multiple HLT filters. The current 2012 data sam-

ples contain several jet triggers at the level of HLT which are presented in Table 1.3 mentioning the trigger thresholds, along with the corresponding L1 trigger seeds. Also the trigger thresholds vs  $p_T$  [4] are shown. As expected,  $H_{T,2}/2$  thresholds ( $|y| < 2.5$ ) are comparable but lower than  $p_T$  thresholds ( $|y| < 3.0$ ). The prescaled low  $p_T$  triggers having different prescales are used to have sufficient data in the lower part of the  $p_T$  spectrum. In addition unprescaled trigger HLT PFJet320 is also used in the region where the jet rate is sufficiently small to collect all the events. During the reconstruction of the spectrum, the prescales have been taken into the account.

Table 1.3: HLT trigger thresholds and corresponding L1SingleJet trigger.

HLT Path	PFJet80	PFJet140	PFJet200	PFJet260	PFJet320
L1 seed	L1SingleJet36	L1SingleJet68	L1SingleJet92	L1SingleJet128	L1SingleJet160
$H_{T,2}/2$ , 99% (GeV)	120.0	187.5	262.5	345.0	405.0
$H_{T,2}/2$ range (GeV)	120 – 188	188 – 263	263 – 345	345 – 406	405 – 480
$p_T$ range (GeV)	133 – 220	220 – 300	300 – 395	395 – 507	507 – 630
Integrated lumi (pb <sup>-1</sup> )	2.12	5.57 x 10	2.61 x 10 <sup>2</sup>	1.06 x 10 <sup>3</sup>	1.97 x 10 <sup>3</sup>

In order to obtain the lower threshold with maximum efficiency of the jet triggers we produce trigger turn on curves for each HLT trigger paths. The efficiency of each trigger is not calculated as a function of jet  $p_T$ , which was used in the trigger decision, but versus  $H_{T,2}/2$ . The triggers show a turn-on behaviour which as can be seen in Figure 1.1.

The trigger efficiency for HLT\_PFJetY is defined as :

$$\text{HLT\_PFJet}_{\text{eff}} Y = \frac{H_{T,2}/2(\text{HLT\_PFJetX} + \text{L1Object\_p}_T > Z + \text{HLTObject\_p}_T > Y)}{H_{T,2}/2(\text{HLT\_PFJetX})} \quad (1.3)$$

Here the denominator represents the number of events for which the trigger path HLT\_PFJetX has been fired. Here the value of X is chosen previous to that of Y in  $p_T$  ordering from the trigger list so that the higher trigger condition can be emulated from the lower trigger path. The numerator is the number of events for which

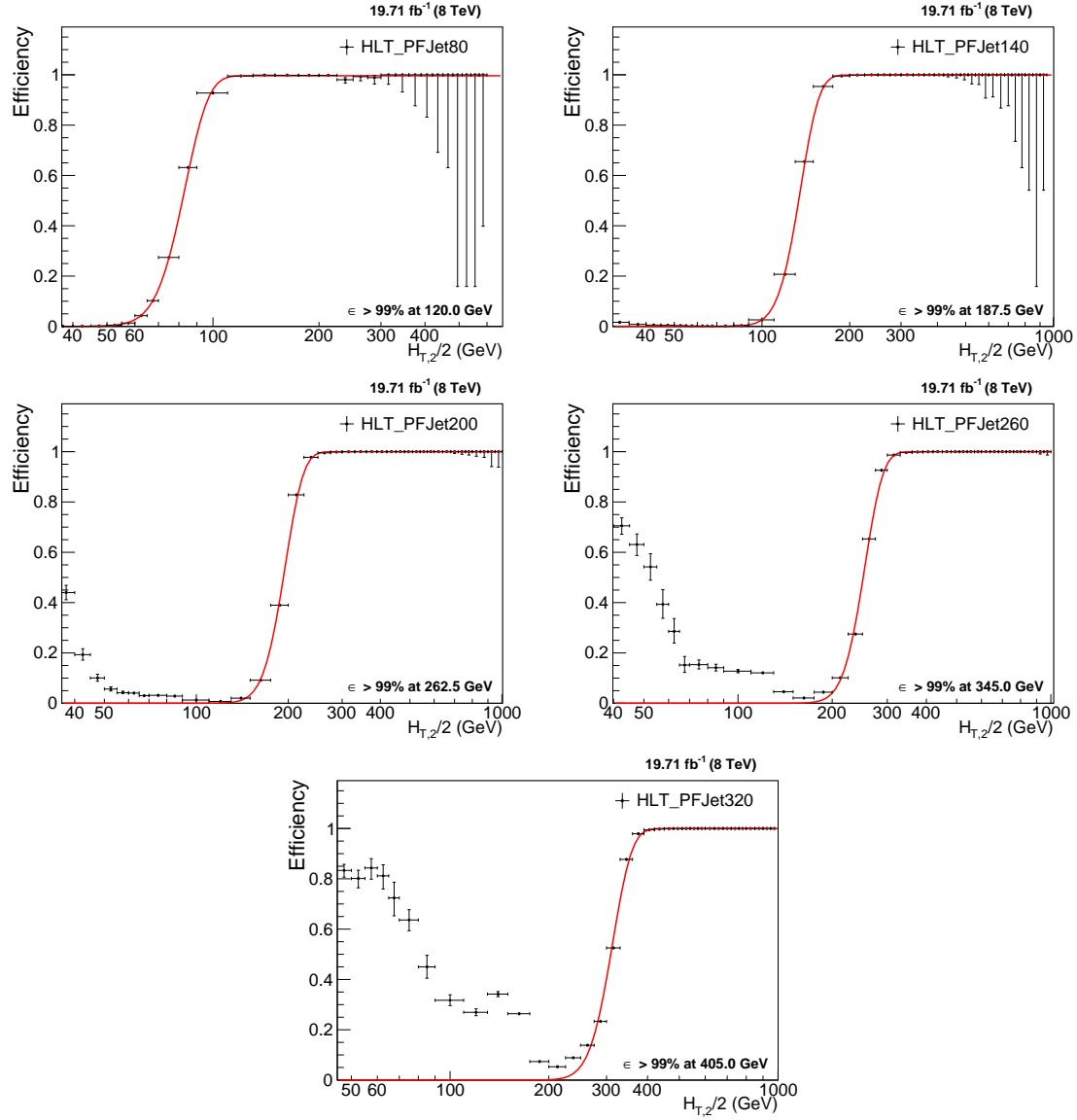


Figure 1.1: Trigger efficiencies turn-on curves for the single jet trigger paths used in the analysis.

HLT\_PFJetX has been fired and the  $p_T$  of L1Object corresponding to the trigger path HLT\_JetX is  $\geq Z$  (where Z is the L1 seed value corresponding to the trigger path HLT\_PFJetY ) and the  $p_T$  of HLTOBJECT corresponding to the trigger path HLT JetX is  $\geq Y$ . For example, in order to obtain turn on curve for HLT\_PFJet260, the immediate HLT path of lower threshold HLT\_PFJet200 is chosen, the  $p_T$  cut on L1Object corresponding to the trigger path HLT PFJet260 is 128 GeV and  $p_T$  cut on HLTOBJECT corresponding to the trigger path HLT Jet260 is 260 GeV. The uncertainty on the efficiency is indicated by error bars which represent Clopper-Pearson confidence intervals. To determine the point, at which the trigger efficiency is larger than 99%, the turn-on distribution is fitted using a sigmoid function, that describes the turn-on behaviour of the trigger paths.

$$f_{fit}(x) = \frac{1}{2} \left( 1 + erf \left( \frac{x - \mu}{\sqrt{2}\sigma} \right) \right) \quad (1.4)$$



# Bibliography

- [1] J. Alwall, M. Herquet, F. Maltoni, O. Mattelaer, and T. Stelzer, “MadGraph 5 : Going Beyond,” *JHEP*, vol. 06, p. 128, 2011.
- [2] T. Sjostrand, S. Mrenna, and P. Z. Skands, “PYTHIA 6.4 Physics and Manual,” *JHEP*, vol. 05, p. 026, 2006.
- [3] J. Alwall *et al.*, “A Standard format for Les Houches event files,” *Comput. Phys. Commun.*, vol. 176, pp. 300–304, 2007.
- [4] C. Collaboration, “Measurement of the double-differential inclusive jet cross section at  $\sqrt{s} = 8$  TeV,” 2015.



*Selected*  
*Reprints*



